First Quarterly Report
for

FEASIBILITY OF GROUND-PENETRATING RADAR FOR USE AT MGP SITES

Richard G. Plumb, Pawan Chaturvedi & Kenneth R. Demarest

Radar Systems and Remote Sensing Laboratory
University of Kansas Center for Research, Inc.
2291 Irving Hill Road, Lawrence, Kansas 66045-2969
913/864-4835 * FAX: 913/864-7789 * OMNET: KANSAS.U.RSL * TELEX: 706352

RSL Technical Report 9990-1

January 1993

Sponsored by:

Electric Power Research Institute
P. O. Box 10412, Palo Alto CA 94303

Agreement RP2879-27

"DISCLOSURE"

This report has not been reviewed to determine whether it contains patentable subject matter, nor has the accuracy of its information or conclusions been evaluated. Accordingly, the report is not considered a published report and is not available for general distribution, and its distribution is limited to employees and advisors of EPRI for the sole purpose of evaluating the progress and the future course of the project described in the report. Until the report has been reviewed and evaluated by EPRI, it should be neither disclosed to others nor reproduced, wholly or partially, without written consent of EPRI.

The University of Kansas, Center for Research Inc.

Table of Content

1. Summary

This is the first quarterly report for the research project, "Feasibility of Ground Penetrating Radar for Use at MGP Sites." During the past two and one half months, an extensive literary survey was done to identify signal processing technique to be used for the project. The technique of Diffraction Tomography is proposed to be used to do the post-processing after the data has been collected using a ground penetrating radar.

Diffraction Tomography is a sophisticated signal processing technique which uses the scattered field data to reconstruct the image of an object buried in an optically opaque medium. This technique has been in use in the field of medical imaging for several years, and is now finding applications in the fields of non-destructive evaluation and subsurface imaging.

In this report, the basic theory of Diffraction Tomography and the problem formulation for this work are described in detail. An algorithm for the implementation of Diffraction Tomography is outlined, and some basic theoretical results are presented.

In the next phase of the project, the Diffraction Tomography algorithm is proposed to be implemented. Finite Difference Time Domain (FD-TD) code is being developed to simulate the scattered fields from the object. The FD-TD technique is a numerical technique for solving for the electric and magnetic field by formulating the Maxwell equations as coupled difference equations. Any inhomogenities can be easily incorporated into the model. This technique would be used to do the simulations and to generate the scattered field data to be used for Diffraction Tomography.

2. Introduction

This is the first quarterly report for "Feasibility of Ground Penetrating Radar for Use at MGP Sites," EPRI Agreement RP2879-27. This report covers the period from September 15, 1992 through December 31, 1992.

The objectives of the first phase of this project were to identify, through literature review, ground penetrating radar (GPR) techniques capable detecting and imaging contaminates at manufactured gas plants (MGP) and other leak sites. We have identified diffraction tomography, an image processing technique, as the leading candidate to image spill sites. Diffraction tomography is a post-processing technique that analyzes the radar data and generates a sub-surface map.

We are preceding to develop a diffraction tomography computer code. This code requires GPR data to image the spill site. To over come the lack of radar data, we are also modifying an existing finite difference - time domain (FD-TD) electromagnetic computer code. The FD-TD algorithm is a very powerful electromagnetic code which will simulate the radar data. We will use FD-TD to generate the signals the radar collects at a spill site. With this code we will be able to model any type of spill located at in any type of background material.

In the following section we outline the basic theory of diffraction tomography. We will wait to the next report to outline the basic theory governing the finite difference - time domain algorithm.

3. Technical Formulation

The fields of non-destructive evaluation and detection of objects buried in opaque media have been the focus of research for many years. Various techniques have been proposed and applied to different problems over the years. The technique to be used for a specific problem depends on the application. Medical imaging, non-destructive evaluation of objects, and subsurface imaging are some of the areas in which these techniques have proved to be extremely useful.

The purpose of this study is to identify and apply a technique for detecting and imaging subsurface contaminates such as leakage from underground storage tanks. These leakages form a plume near the storage tank and contaminate the surrounding area. The existing techniques involve digging core samples from the surrounding area and analysing them. The use of a ground penetrating radar is proposed to take the measurements of the scattered field which are to be utilized in the imaging technique.

For subsurface imaging, two of the most powerful techniques currently used are those of holography and diffraction tomography. In holographic techniques, the underground object is imaged by measuring the reflected field at the surface of ground. Fresnel-Kirchoff or Fraunhoffer diffraction theory is used for the analysis and the development of the reconstruction algorithms for microwave holography [1],[2],[3]. In this technique, a Synthetic Aperture Radar or a pulsed radar is used and the image of the object is computed from the correlation between the received signal and a reference signal. The object information is recorded as an interference pattern between an illuminating wave which is identical to the reference signal, and the wave scattered by the object being imaged. This interference pattern is known as a hologram. The illumination of this pattern by the reference signal produces a real and a virtual image of the object. This technique is usually used with higher frequencies. Since the signal used for reconstruction of subsurface objects is the signal reflected from the object, best results are achieved with metallic or other objects which result in strong scattering.

Diffraction tomography is the generalization of the computer tomography technique which has been in use in medical imaging for several years. The diffraction effects are incorporated to account for the lower frequencies used in these applications. The image is reconstructed by taking the projections of the object for various angles of incidence.

Computer Tomography can loosely be defined as the technique of reconstructing the image of an object embedded in an optically opaque background from the slices of the image which

represent the projections of the object. These slices of the image are obtained by measuring the effect of the object on an applied field. Using this technique, an N-dimensional object, which can be represented by its N-dimensional Fourier transform, can be reconstructed from the (N-1)-dimensional Fourier transforms of its projections [3],[4],[5]. For the case of a 2-dimensional object, the Fourier transform of the field taken along a line represents the Fourier transform of the projection of the object along that line. By measuring these projections of the object along different lines (directions), the object can be reconstructed from these 1-dimensional Fourier transforms. The applications of tomography can be broadly classified into two major areas, medical tomography and goephysical tomography.

The depth of penetration required for this project necessitates the use of lower frequencies because of the high attenuation at higher frequencies for wave propagation in ground. This, combined with the fact that tomographic techniques result in better quality of objects buried in attenuating media when the contrast between the object and the background medium is not very high, makes tomography a more appropriate technique for this application. The issues of resolution and frequency of operation are discussed in detail in a later section.

The technique of Computer Tomography has been applied to medical imaging for several years. The field of medical tomography has been well studied. In medical applications, since the depth of penetration required is not very large and thus attenuation in the object does not pose a severe limitation, X-rays are used to reconstruct the image. Because of the high frequencies used, diffraction effects can be neglected and the straight-ray models work reasonably well. Using these models, the Fourier transform of the field along a direction perpendicular to the direction of the incident wave gives the Fourier transform of a slice of the object along this direction according to the projection slice theorem as shown in Fig. 1. By rotating the transmitter and the receiver 360 degrees around the object, if sufficient number of measurements are made, the object can be reconstructed from these slices.

The application of the tomographic techniques to geophysical problems is relatively new and is not as well documented. In geophysical applications, the simple straight-ray models cannot be applied because of the high attenuation suffered by the higher frequencies [4]. This necessitates the use of lower frequencies. At lower frequencies, the diffraction effects play an important part and can no longer be neglected. Another problem in geophysical tomography is the inhomogeneity of the background medium. Further, unlike medical tomography, the view angles available are limited since the transmitter and the receiver cannot be rotated 360 degrees around the object.

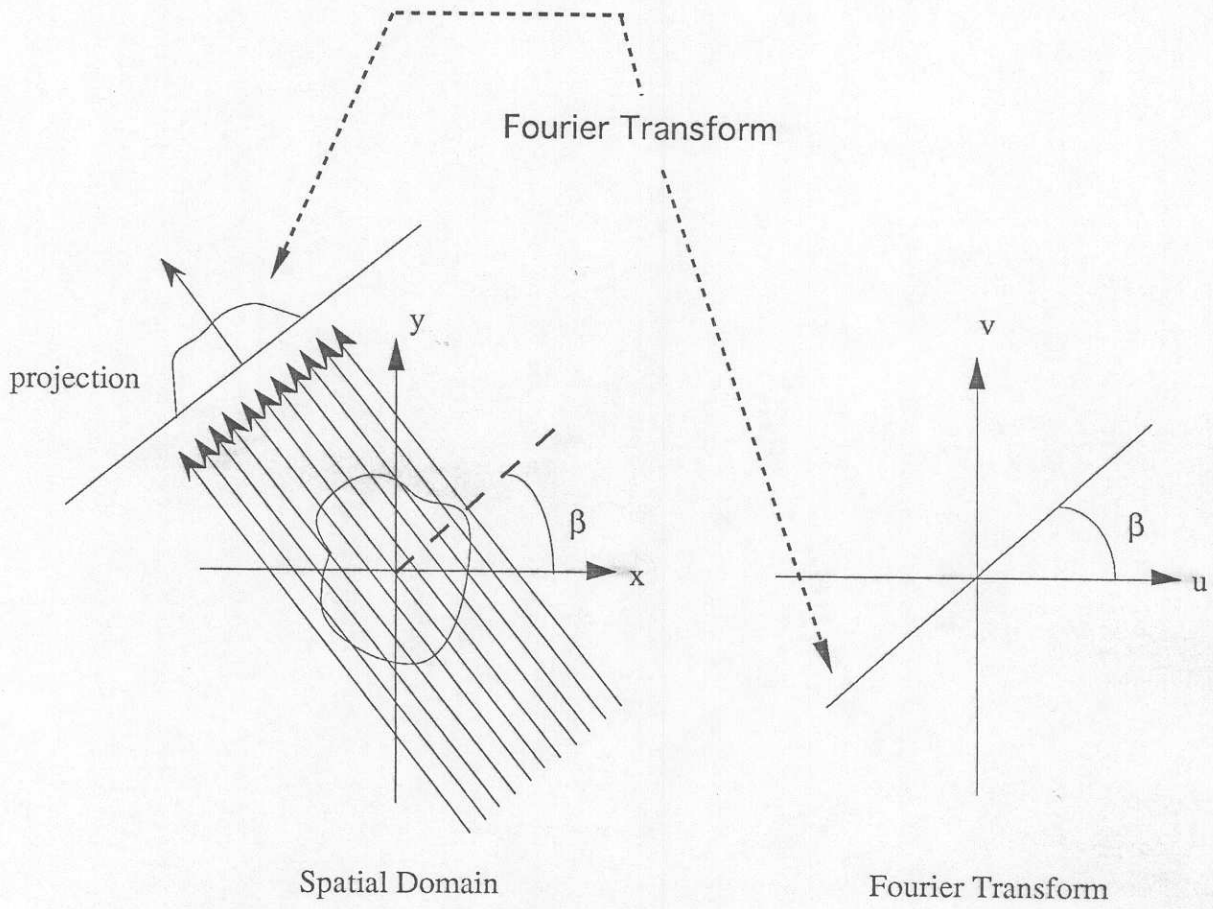

Fig. 1. The projection slice theorem in medical tomography

Because of the limited availability of the viewing angles, and the presence of diffraction effects, the geophysical tomographic analysis and its applications are more complicated than the medical tomographic applications. In the presence of diffraction effects, the problem of geophysical tomography reduces to solving a nonlinear inverse scattering problem. Simplifying assumptions are made about the scattering properties of the object to solve the problem. These include the assumption of a homogeneous background, and the weak scattering model (Born or Rytov Approximation). The weak scattering model works well even in the presence of a single strong scatterer.

In this project, geophysical tomography techniques are used to reconstruct the image of the spill from the underground tank at a depth of a few meters below the surface. Since the frequencies used cannot be very high, diffraction tomography has to be applied for this problem. For diffraction tomography, a result similar to the projection slice theorem of medical tomography can be stated as follows [4],[5],[6]: The 2-dimensional Fourier transform of the object along a

semicircular arc is related to the Fourier transform of the scattered field along a straight line tangential to the arc as shown in Fig.2. This result can be utilized with forward and back-scattering to reconstruct the image of the object from the 1-dimensional Fourier transforms.

One of the most popular techniques used for this class of problems is the back-propagation algorithm proposed by Devaney[4]. But due to the use of spatial filtering operation utilized for image reconstruction by this algorithm, it is computationally very intensive. A direct interpolation scheme has been used by some people to solve similar problems [7]. A similar interpolation based algorithm is used here to solve the problem. The interpolation scheme is modified to make it applicable to the back-propagation case for geophysical tomography.

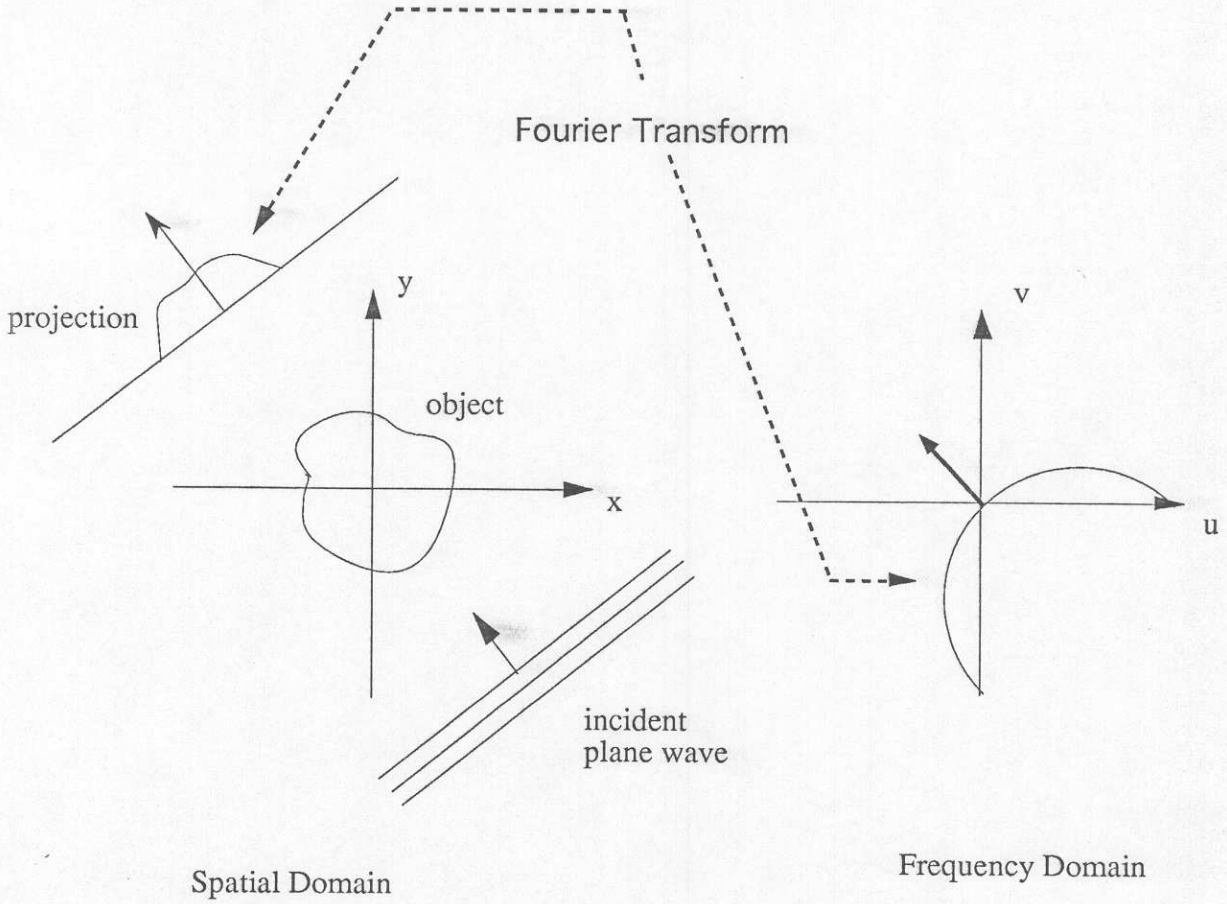

Fig. 2. The relationship between Fourier transforms of the object and the scattered field for diffraction tomography.

I. Problem Formulation

For geophysical tomography, the transmitters and the receivers can be arranged in three possible configurations. One way is to have either the transmitters on the surface of the ground and the receivers in a borehole or the transmitters in the boreholes and the receivers on the surface. This is known as the offset VSP (vertical seismic profiling) configuration. Another possibility is to have both the transmitters and the receivers in boreholes around the object. This is known as the borehole-to-borehole configuration. A third arrangement is to have both the transmitters and the receivers on the surface. It is observed that borehole-to-borehole arrangement gives a better coverage of the object in the k-space. Since the quality of the reconstructed image is directly related to the k-space coverage, better images can be achieved with this arrangement. But for geophysical applications, offset VSP provides an arrangement which is easier to implement, and results in images of satisfactory quality for most applications. For the work presented here, the VSP arrangement has been used for this reason, but the results can be used for the other configurations also. The issue of k-space coverage is discussed more elaborately in a later section.

A. Plane Wave Synthesis

Consider the offset VSP arrangement, with the receivers located at x=l as shown in Fig.3 and the sources located on the surface of ground. If the sources are line sources, each source will generate a cylindrical wavefront propagating downwards. Sincethe incident wave is assumed to have a plane wavefront in tomographic analysis these wavefronts need to be combined to obtain a plane wavefront. This can be achieved by a process similar to slant-stacking used in geophysics. Instead of having all the sources emit at the same time, a technique similar to the one used in synthetic-aperture radars can be used to generate a plane wave using just one source. The waves from the source at different source locations along a straight line on the surface can be added, with the phase varying linearly along the line of transmitter locations. The waves are combined at the receivers to synthesize plane waves at the receiver.

Let the number of transmitter locations be N, located along a straight line on the surface from left to right. Let the transmitter spacing be "d" and the incident wavevector be $\mathbf{k} = k\mathbf{s_0}$ which makes an angle ϕ with the positive x-axis. $\mathbf{s_0}$ is a unit vector along the direction of the incident wavevector. If the additional distance travelled by the wave transmitted from the n^{th} location compared to the wave transmitted from the $(n-1)^{th}$ location is ΔR, the phase difference between signals from these two successive transmitter locations $\Delta\phi$ can be written as

$$\Delta\phi = \frac{2\pi}{\lambda}\Delta R = \frac{2\pi}{\lambda} d \cos\phi = d\,\mathbf{k}\cdot\mathbf{x} \qquad (1)$$

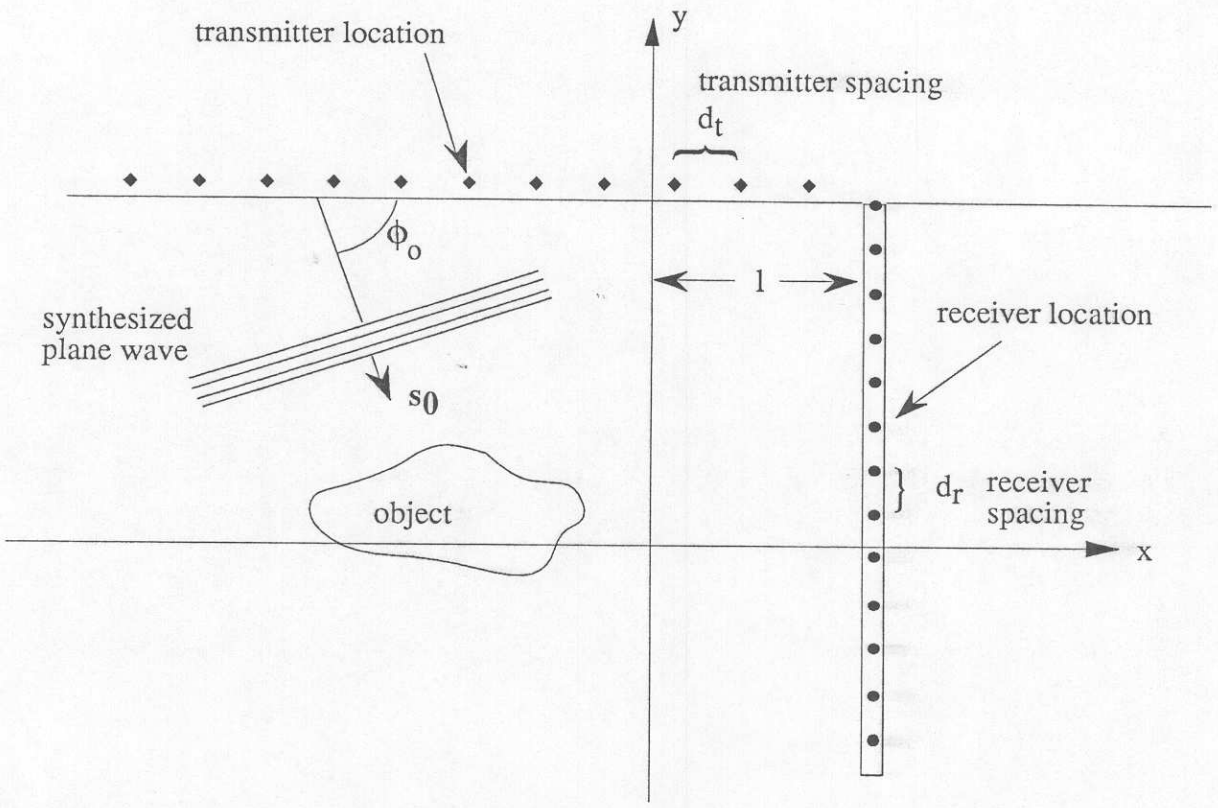

(a)

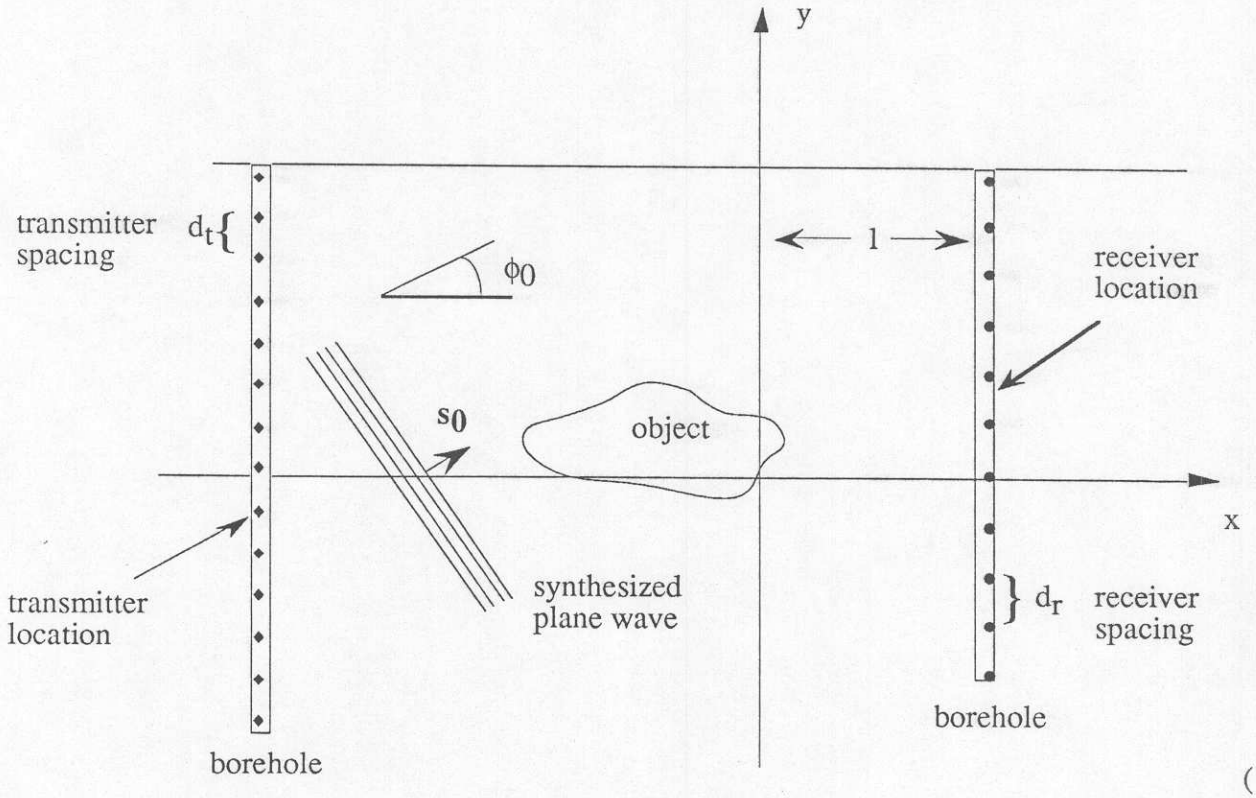

b)

Fig. 3.(a) Offset VSP and (b) Borehole-to-borehole tomography

where $\mathbf{k}\cdot\mathbf{x}$ represents the scalar dot product between the vector $\mathbf{k}$ and the unit vector $\mathbf{x}$ which points along the direction of positive x-axis. The surface of ground is assumed to be parallel to the x-axis. The scattered field at the i^{th} receiver due to the synthesized plane wave is then given by

$$S_i = \sum_{n=0}^{N-1} Y_{in} \exp(jn\Delta\phi) \tag{2}$$

where Y_{in} is the measurement at the ith receiver when the transmitter is at the location n, and S_i is the plane wave response at the receiver location i. Using this synthesized plane wavefront, the equations required for image reconstruction can be formulated.

B. Diffraction Tomography

A 2-dimensional electromagnetic scattering problem can be solved by considering the scalar wave equation instead of the vector wave equation. Using the scalar wave model, and considering a 2-dimensional object, the time dependent wavefield satisfies the inhomogeneous Helmholtz equation. Thus the Fourier amplitude of the time dependent wavefield $u_t(\mathbf{r}, \omega)$ will also satisfy the inhomogeneous equation

$$(\nabla^2 + k^2) u_t(\mathbf{r}, \omega) = -o(\mathbf{r}, \omega) u_t(\mathbf{r}, \omega) \tag{3}$$

where $u_t(\mathbf{r}, \omega)$ represents the Fourier transform of the z-component of the total electric field. $o(\mathbf{r}, t) = k^2 - k_0^2$ is the object profile and it has a 2-dimensional Fourier transform

$$O(\mathbf{r}, \omega) = \int_{-\infty}^{+\infty} o(\mathbf{r}, t) \exp(-j\,\omega\, t)\, dt \tag{4}$$

The incident plane wave is of the form

$$u_i(\mathbf{r}) = U_0(t) \exp(j\, k\, \mathbf{s_0}\cdot\mathbf{r}) \tag{5}$$

where U_0 is the complex amplitude at the origin, and k is the wavenumber in the background medium. Since the total field at any point in space can be written as a sum of the incident field and the scattered field,

$$u_t(\mathbf{r}, \omega) = u_i(\mathbf{r}, \omega) + u_s(\mathbf{r}, \omega) \tag{6}$$

Let the spatial Fourier transform at $\mathbf{r} = \mathbf{r_0}$ (x=l, y) of the total, incident, and the scattered field, $U(\kappa, \omega)$, $U_i(\kappa, \omega)$ and $U_s(\kappa, \omega)$ respectively, be defined as

$$U_m(\kappa, \omega) = \int_{-\infty}^{+\infty} u_m(y, \omega) \exp(-j\, \kappa\, y)\, dy \qquad m = i, s, t$$

The Helmholtz equation can be simplified using the Green's function. Using the boundary conditions and converting the differential equation of (3) into an integral equation, the Fourier transform of the total field can be expressed as

$$u_t(\mathbf{r}, \omega) = U_0(\omega) \exp(j\, k\, \mathbf{s_0}\cdot\mathbf{r}) + \int O(\mathbf{r}', \omega)\, u_t(\mathbf{r}', \omega)\, G'(|\mathbf{r} - \mathbf{r}'|)d\mathbf{r}' \qquad (7)$$

where $G'(|\mathbf{r} - \mathbf{r}'|)$ is the Green's function for Eq.(3) in the absence of the scattering object. The Green's function is

$$G'(|\mathbf{r} - \mathbf{r}'|) = \frac{-j}{4} H_0^{(2)}(k|\mathbf{r} - \mathbf{r}'|) \qquad (8)$$

where $H_0^{(2)}(k|\mathbf{r} - \mathbf{r}'|)$ is the zero order Hankel function of the second kind. The vector $\mathbf{r}'=x'\mathbf{x}+y'\mathbf{y}$ represents the source vector, and $\mathbf{r}=x\mathbf{x}+y\mathbf{y}$ represents the field vector. The plane wave expansion of the Hankel function $H_0^{(2)}(k|\mathbf{r} - \mathbf{r}'|)$ along the line of observation $\mathbf{r}=\mathbf{r_0}=l\mathbf{x}+y\mathbf{y}$ is given by

$$H_0^{(2)}(k|\mathbf{r} - \mathbf{r}'|) = \frac{1}{\pi\gamma} \int_{-\infty}^{+\infty} \exp[j\, \{\kappa\, (y - y') + \gamma\, (l - x')\}]\, d\kappa \qquad (9)$$

where

$$\kappa^2 + \gamma^2 = k^2 \qquad (10)$$

For a general wavevector $\mathbf{k}$, κ and γ represent the components of $\mathbf{k}$ along two orthogonal directions. The physical meaning of these two components in the context of this problem is explained in more detail in the next section. Substituting Eq.(8) into Eq.(7)

$$u_t(\mathbf{r}, \omega) = U_0(\omega) \exp(j\, k\, \mathbf{s_0}\cdot\mathbf{r}) + \frac{-j}{4} \int O(\mathbf{r}', \omega)\, u_t(\mathbf{r}', \omega)\, H_0^{(2)}(k|\mathbf{r} - \mathbf{r}'|)d\mathbf{r}' \qquad (11)$$

The first term represents the incident field, and the second term is due to the scattering by the object. Eq. (11) expresses the total field in terms of the incident field and the scattered field due to the presence of the object with the profile O. Since the total field u_t depends on the object profile

O, the second term on the right hand side of Eq.(11), which has both the object profile and the total field inside the integral, makes this equation a non-linear equation in the object profile O.

II. Solution Techniques

The direct scattering problem consists of solving the non-linear equation (11) for the total field u_t for a given object profile. In the inverse problem, Eq.(11) is solved for the object profile when a set of field measurements is given. Thus the inverse scattering problem in geophysical tomography consists of evaluating the object profile from a set of measurements of the total field along a fixed line x=l for different angles of incidence.

This problem is difficult to solve in a closed form without any simplifications. But by making the assumption that the scattered field is small compared to the incident field, equation (11) can be solved for the object profile. Since this assumption is equivalent to assuming that the object is a weak scatterer, it is known as the weak scattering approximation. The assumption of weak scattering can be incorporated here into the problem by using either the first order Born approximation or the Rytov approximation. The first order Born approximation consists of approximating the total field on the right hand side of Eq.(11) by only the incident field, i.e., by assuming the effect of the second term on the total field to be small compared to the contribution from the incident field. This assumption would be valid if both the magnitude of the object profile and the total object volume are small. This gives the field at the line of observation $\mathbf{r}_0$(x=l) as

$$u(\mathbf{r}_0, \omega) = U_0(\omega) \exp(j\, k\, \mathbf{s}_0 \cdot \mathbf{r}_0) - \frac{j}{4} U_0(\omega) \int O(\mathbf{r}', \omega) \exp(j\, k\, \mathbf{s}_0 \cdot \mathbf{r}') H_0^{(2)}(k|\mathbf{r}_0 - \mathbf{r}'|) d\mathbf{r}' \qquad (12)$$

Instead of using the Born approximation, which is a Taylor series expansion for a small object profile, the Rytov approximation can be used. Rytov approximation is a less restrictive condition and has been reported to give better results. For the Rytov approximation, the total field is expressed as [10]

$$u(\mathbf{r}, \omega) = U_0(\omega) \exp(j\, \mathbf{k} \cdot \mathbf{r} + j\, \psi(\mathbf{r}, \omega)) \qquad (13)$$

where $\psi(\mathbf{r}, \omega)$ is the perturbation on the complex phase of the signal and it has a spatial Fourier transform $\psi(\kappa, \omega)$ at $\mathbf{r} = \mathbf{r}_0$. In the Rytov approximation, the effect of scattering is included in the complex phase, which is expressed as $\mathbf{k} \cdot \mathbf{r} + \psi(\mathbf{r}, \omega)$. The perturbation term for the Helmholtz Eq.(3) under the Rytov approximation is given by

$$\psi(\mathbf{r}, \omega) = \frac{-j}{u_i(\mathbf{r}, \omega)} \int O(\mathbf{r}', \omega)\, u_i(\mathbf{r}', \omega)\, G'(k|\mathbf{r} - \mathbf{r}'|) d\mathbf{r}' \qquad (14)$$

Substituting Eq.(8) in (14)

$$\psi(\mathbf{r}, \omega) = \frac{-1}{4} \exp(-j\, k\, \mathbf{s_0}\cdot\mathbf{r}) \int O(\mathbf{r}', \omega) \exp(j\, k\, \mathbf{s_0}\cdot\mathbf{r}')\, H_0^{(2)}(k|\mathbf{r} - \mathbf{r}'|)d\mathbf{r}' \qquad (15)$$

The field along the line of observation is obtained by substituting $\mathbf{r} = \mathbf{r_0}$. Eq.(12) and (15) represent the relationship between the object and the scattered field for the Born and Rytov approximations respectively. Note that the integrals in both the equations are the same. Denoting the integral by 2 $Q_\phi(y, \omega)$, where the subscript ϕ represents the angle of incidence of the plane wave,

$$Q_\phi(y, \omega) = \frac{-1}{2} \int O(\mathbf{r}', \omega) \exp(j\, k\, \mathbf{s_0}\cdot\mathbf{r}')\, H_0^{(2)}(k|\mathbf{r}_0 - \mathbf{r}'|)d\mathbf{r}' \qquad (16)$$

y is used in place of $\mathbf{r}$ in the argument of Q_ϕ since the x coordinate is fixed (x=l) at $\mathbf{r} = \mathbf{r_0}$. In the above equation, $Q_\phi(y, \omega)$ represents the data which is used for the evaluation of the object profile. Substituting the Hankel function expansion from Eq.(9) in (16)

$$Q_\phi(y, \omega) = \int \frac{1}{2\pi\gamma} \int_{-\infty}^{+\infty} \exp[j\, \{\kappa\,(y - y') + \gamma\,(1 - x')\}].$$
$$O(\mathbf{r}', \omega) \exp(j\, k\, \mathbf{s_0}\cdot\mathbf{r}')\, d\kappa\, d\mathbf{r}' \qquad (17)$$

Eq.(17) can be rearranged as

$$Q_\phi(y, \omega) = \frac{\exp(j\,\gamma\, l)}{\gamma} \frac{1}{2\pi} \int \exp(j\,\kappa\, y)\, d\kappa$$
$$\{ \int_{-\infty}^{+\infty} \exp[j\, ((k s_{0y} - \kappa)\, y' + (k s_{0x} - \gamma)\, x')]\, O(\mathbf{r}', \omega)\, d\mathbf{r}' \} \qquad (18)$$

The first integral represents the inverse spatial Fourier transform of the term in the curly brackets. Define a new vector $\mathbf{w}$ as

$$\mathbf{w} = k\,(\mathbf{s} - \mathbf{s_0}) \qquad (19)$$

where $\mathbf{s}$ is a unit vector defined as

$$\mathbf{s} = \frac{1}{k}(\gamma\,\mathbf{x} + \kappa\,\mathbf{y}) \qquad (20)$$

Eq.(20) defines κ and γ as the y- and x- components respectively of the wavevector $k\mathbf{s}$. The locus of points defined by $\mathbf{w}$ is a semicircle of radius k and centered at $-k\mathbf{s_0}$. Taking the Fourier transform of $Q_\phi(y, \omega)$ from Eq.(18),

The 1-dimensional Fourier transform of the field is related to the 2-dimensional Fourier transform of the object taken along the semicircles defined by Eq.(19) by [7]

$$O(\mathbf{w}) = \begin{cases} \dfrac{j\,2\,\gamma\,\exp(-j\,\gamma\,l)}{U_0}\,U_s(\kappa) & \text{for Born Approximation} \\ 2\,\gamma\,\exp[-j(\gamma - ks_{0x})l]\,\psi(\kappa - ks_{0y}) & \text{for Rytov Approximation} \end{cases} \tag{22}$$

where the argument ω has been dropped for notational convenience without any loss of information.

From Eq.(22), it can be seen that the 1-dimensional Fourier transform of the field taken along the line x=l is related to the 2-dimensional Fourier transform of the object profile taken along a semicircle of radius k and centered at $-ks_0$. This represents the basic result of diffraction tomography. Thus, by measuring the scattered field for many different angles of incidence, the Fourier transforms of the object are obtained along the corresponding semicircles. The object profile can then be reconstructed from the scattered field. Fig. 4 shows three such semicircles for $\phi = 0, -\pi/2$, and $-\pi$. For the case of offset VSP, the angles ϕ would vary from 0 to $-\pi$. So the points in the k-space at which the data is available would all lie on semicircles which have their centers in the first or the second quadrant. For each value of ϕ, there will be a different semicircle. Note that tangents to all the semicircles are parallel to the line of observation. γ and κ can be seen as the projections of the wavevector ks on the x- and y-axis respectively.

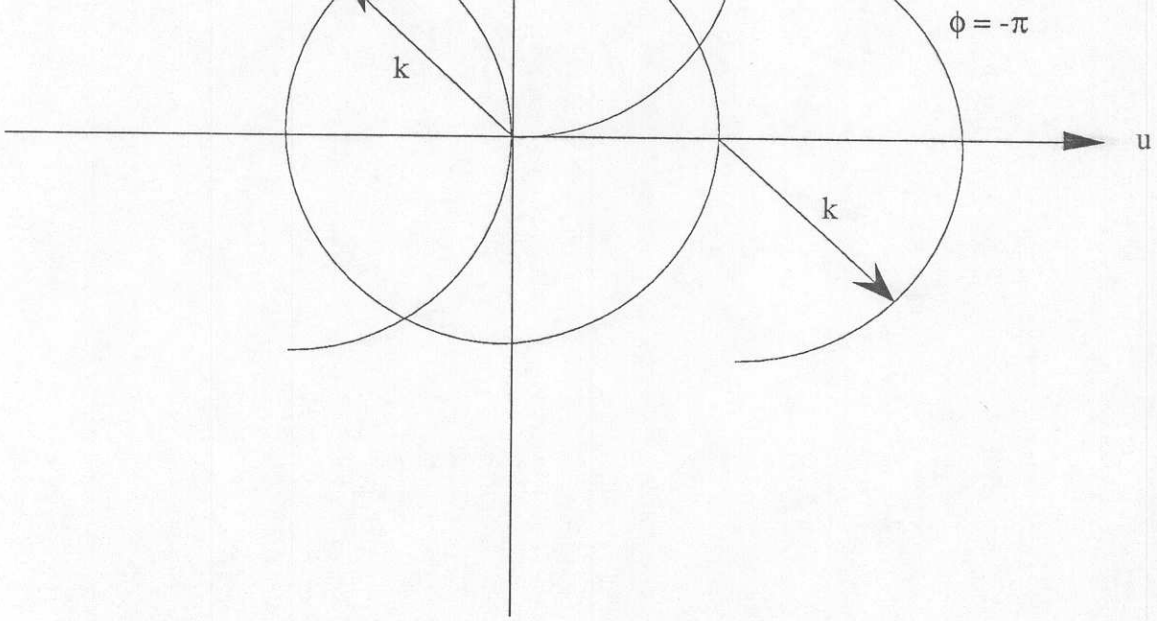

Fig. 4. The semicircles in k-space over which the Fourier transform of the object is obtained.

The points along the other half of the circles can be obtained if there is a set of receivers on the other side of the transmitter locations (x=-l). From this analysis, it can also be seen that the object coverage would be better for two boreholes at $x=\pm 1$ with set of transmitter locations on the surface. The k-space coverage for the various cases is shown in Fig.5. Note that the centers of all the semicircles lie on a circle of radius k and centered at the origin of the k-space as shown in Fig.4. This implies that even if measurements could be made along all possible orientations of the receiver array for various angles of incidence ϕ, the coverage in k-space would still be limited to a circle of radius 2k. This results in a loss of the sharper features which correspond to higher spatial frequencies during reconstruction of the image.

For the case of weakly scattering objects, most of the scattered field would lie in the forward direction. This is another reason for the image quality being better for offset VSP and borehole-to-borehole arrangements, as compared to the the case when the transmitters and the receivers are both on the surface of ground. Although the best image quality would be achieved with borehole-to-borehole tomography, having receivers in two boreholes on either side of the object significantly improves the k-space coverage for offset VSP, which results in better image quality. For most applications for which weak scattering approximation is valid, the standard offset VSP arrangement provides images of sufficient quality and a simpler practical implementation. This was the reason for the selection of offset VSP as the scheme used for this work. It should be noticed here that for a strong scatterer, since most of the scattered field would lie in the backward direction, having both the transmitters and the receivers on the surface may provide the best images even though the k-space coverage is lesser than in the case of the other arrangements.

In the case of medical tomography, the transmitted plane wave and receiver array are always parallel to each other, but the receiver axis itself rotates around the object. This results in tangents to all the semicircles passing through the origin in k-space for all values of ϕ. This would

It is interesting to note that the cases of forward and reflection tomography are complementary to each other in the sense that the data obtained in the two cases is along the two complementary semicircles which constitute the full circle for any given direction.

From the above discussion, it is apparent that the image obtained by using diffraction tomography would be inherently a low pass version of the object. Further, the image quality would be poorer in the regions of lower k-space coverage. The k-space coverage would depend directly on the frequency of operation. In geophysical applications, since attenuation imposes a limit on the frequency, image quality has to be sacrificed. But even with this limitation, images of sufficient quality can be obtained. However, it is important to choose a high enough frequency to satisfy the resolution criterion and to sample along the receiver axis at a rate higher than the Nyquist rate.

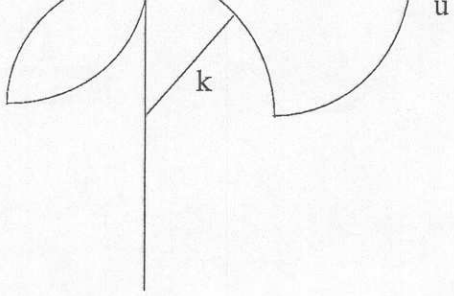

Offset VSP

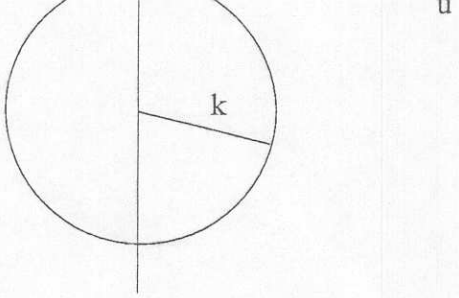

Borehole-to-borehole

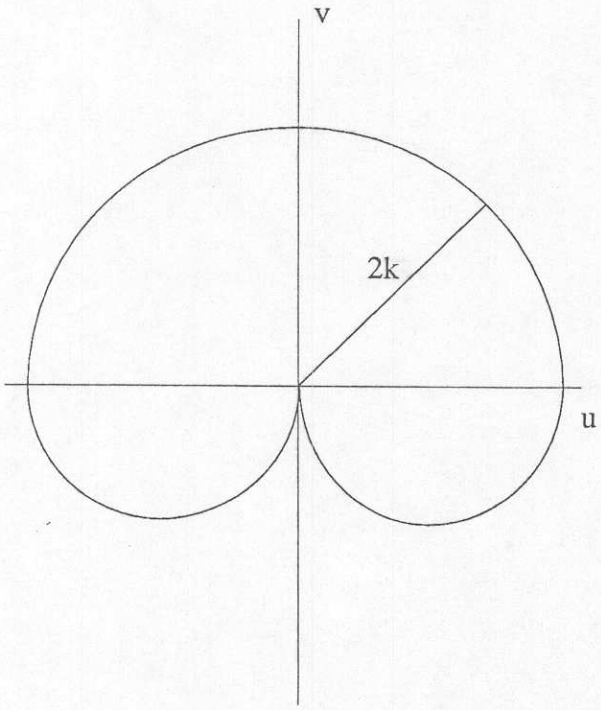

Offset VSP with two boreholes

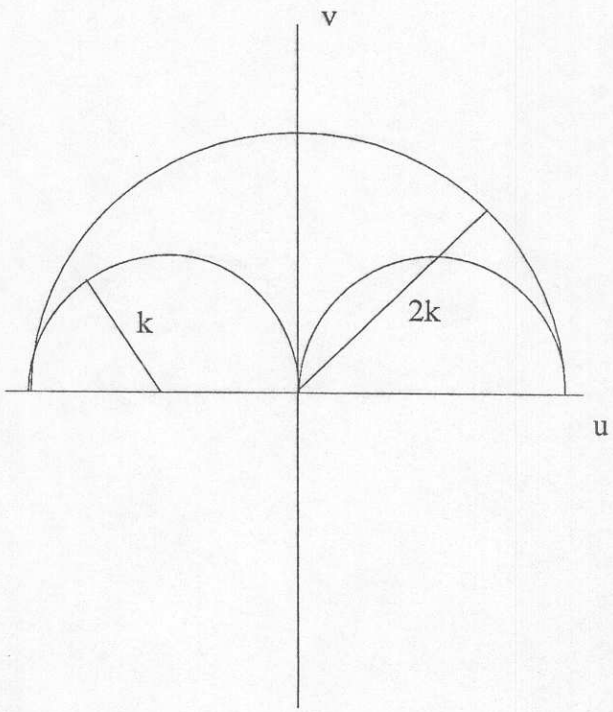

Transmitter and receivers
both on the surface

Fig.5. The k-space coverage for various cases for a complex profile.

propagate the field backwards into the object. For each measurement, the spatial filter is applied to the data and the results of all these operations are combined to form the image of the object. But because of the use of the spatial filter at each step of reconstruction, this algorithm is computationally intensive. Since the amount of computation would have a direct bearing on the speed of the algorithm, and hence on the practical implementation of the algorithm, a computationally faster algorithm is desirable. Direct interpolation approach was chosen for this work for the same reason.

All the calculations are performed in the Fourier space in the direct interpolation based algorithms. As seen earlier, the field measurements are related to the object profile in Fourier space by Eq.(22). The image of the object can in principle be obtained by Fourier inversion of the data. Before going on to reconstruct the object, it is necessary to convert the data which is obtained over a grid of semicircles to points on a rectangular coordinate system. The image can then be obtained by a direct Fourier inversion of these points. A direct transformation scheme is derived here to convert the data points from a semicircular grid to a rectangular coordinate system (u,v). This transformation is similar to the coordinate transformation used for the case of forward tomography.

A. Coordinate Transformation

Let each point on the semicircular grid be defined by its (κ, ϕ) coordinates where κ is the projection of the scattered wavevector on the y-axis as defined in Eq.(10), and ϕ is the angle that the incident wavevector makes with the positive x-axis, as mentioned earlier. Thus each set of incident and scattered wavevectors can be uniquely identified by its κ and ϕ coordinates. Note that the κ and ϕ values do not represent the polar coordinates. As the angle ϕ is varied over the range of allowed values, κ can take values between -k and +k. The cases of negative and positive values of κ need to be treated separately as they result in slightly different transformation equations.

$$\cos(\beta - \theta) = \frac{w}{2k} \tag{26}$$

This implies

$$\beta = \tan^{-1}\left(\frac{v}{u}\right) + \cos^{-1}\left(\frac{\sqrt{u^2 + v^2}}{2k}\right) \tag{27}$$

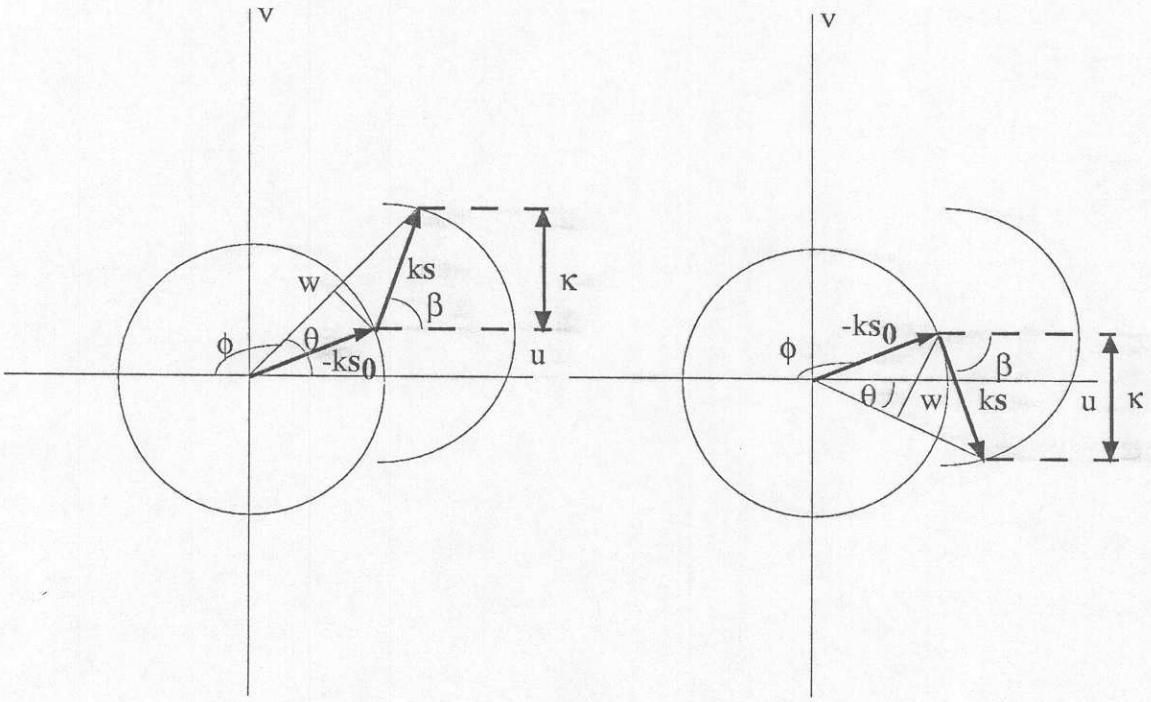

(a) $0 < \kappa < k$ (b) $-k < \kappa < 0$

Fig. 6. The geometry for the coordinate transformation.

This gives

$$\phi = \pi + \cos^{-1}\left(\frac{\sqrt{u^2 + v^2}}{2k}\right) - \tan^{-1}\left(\frac{v}{u}\right) \tag{29}$$

Eqs.(28) and (29) give the desired transformation from (κ, ϕ) coordinates to (u, v) coordinates for $0<\kappa<k$. For $-k<\kappa<0$, from Fig.6(b),

$$\kappa = -k \sin \beta \tag{30}$$

$$\theta = \tan^{-1}\left(\frac{v}{u}\right) \tag{31}$$

and

$$\cos(\beta + \theta) = \frac{w}{2k}$$

or

$$\beta = \cos^{-1}\left(\frac{\sqrt{u^2 + v^2}}{2k}\right) - \tan^{-1}\left(\frac{v}{u}\right) \tag{32}$$

Substituting Eq.(32) into (30),

$$\kappa = -k \sin\left\{\cos^{-1}\left(\frac{\sqrt{u^2 + v^2}}{2k}\right) - \tan^{-1}\left(\frac{v}{u}\right)\right\} \tag{33}$$

The expression for ϕ in terms of u and v is given by

$$\pi - \phi = \beta + 2\theta$$

or

$$\phi = \pi - \beta - 2\theta$$

which gives

$$\phi = \pi - \cos^{-1}\left(\frac{\sqrt{u^2 + v^2}}{2k}\right) - \tan^{-1}\left(\frac{v}{u}\right) \tag{34}$$

Eqs.(33) and (34) give the transformation for negative values of κ. It is apparent from Eq.(23) and (30) that κ always lies between -k and k for all real values of k. Eq.(28), (29), (33) and (34) define a one-to-one transformation between the (κ, ϕ) and (u, v) coordinates.

Bilinear interpolation is one of the most popular techniques used for generating the missing data for image reconstruction and is the technique which is proposed to be used in this work. Although this technique also has the interpolation errors associated with other interpolation schemes, it appears to give fairly good results for image reconstruction using diffraction tomography. A very brief description of the bilinear interpolation technique used is presented here. The reader may refer to [7] and [8] for a detailed description of this material.

The operation of bilinear interpolation can be represented by a filtering operation. For image reconstruction using Eq.(21) and (22), $O(w)$ is directly related to the data $Q_\phi(\kappa)$. The transmitted plane waves would be uniformly spaced in the angular coordinate ϕ. Further, since the receiver spacing is uniform along the y-axis, the data would also be uniformly spaced in κ. Thus the data obtained would be uniformly spaced in the (κ, ϕ) coordinates, which would result in non-uniform sampling on the semicircular arcs. The bilinearly interpolated values of the function $Q_{\phi_j}(\kappa_i)$, given $N_\kappa \times N_\phi$ uniformly spaced samples of this function, are given by

$$Q_\phi(\kappa) = \sum_{i=1}^{N_\kappa} \sum_{j=1}^{N_\phi} Q_{\phi_j}(\kappa_i)\, h_1(\kappa - \kappa_i)\, h_2(\phi - \phi_j) \tag{35}$$

where

$$h_1(\kappa) = \begin{cases} 1 - \dfrac{|\kappa|}{\Delta\kappa} & |\kappa| \le \Delta\kappa \\ 0 & \text{otherwise} \end{cases} \tag{36}$$

and

$$h_2(\phi) = \begin{cases} 1 - \dfrac{|\phi|}{\Delta\phi} & |\phi| \le \Delta\phi \\ 0 & \text{otherwise} \end{cases} \tag{37}$$

$\Delta\kappa$ and $\Delta\phi$ are the sampling intervals for κ and ϕ respectively.

have an effect on the quality of the reconstructed image. Since the basic assumption made in the analysis of diffraction tomography and object reconstruction is the validity of the Born or Rytov approximation, this technique works best for the case when the scattering by the object is weak. However, it would also work well for the case of an isolated scatterer. This performance of this technique is not known for the case when the area being imaged has multiple strong scatterers. This provides the most severe limitation on image reconstruction using this technique.

Even when the weak scattering approximation is valid, since the image obtained is inherently a low pass version of the object, there is a loss of the sharp features of the object [8]. The k-space coverage can be increased by using higher frequencies, but in geophysical applications, the attenuation increases significantly at higher frequencies. This imposes a limitation on the maximum frequeny that can be used.

For a given frequency, there are gaps in the k-space coverage provided by the offset VSP configuration. These gaps in the k-space coverage result in artifacts along this direction. The image quality can be significantly improved by placing receivers on both sides of the object, thus eliminating these gaps in the coverage. However, the offset VSP gives images of sufficient quality despite lower k-space coverage.

In view of all these limitations, the parameter selection for diffraction tomography is of critical importance [8]. By the right selection of parameters, the image quality can be significantly enhanced.

The frequency of operation has a direct bearing on the resolution. It has been observed that to resolve a feature of spatial extent R, the wavelength has to be less than approximately four times R, i.e,

$$\frac{R}{\lambda} \geq 0.25 \tag{38}$$

A similar condition needs to be satisfied for the number of plane waves generated. Since the image is periodic in the angular coordinate ϕ with period 2π, the minimum number of distinct plane waves required to reconstruct the object can be obtained from the circular sampling theorem [9]. If K is the highest angular frequency in the object, the object can be reconstructed from the data if there are at least $(2K + 1)$ samples in each period. In case of objects having an infinite or very large K, an approximate value of K can be obtained which will result in satisfactory image quality.

If 2A is the spatial extent of the object, the maximum cartesian grid spacing in frequency is $\Delta u = 1/(2A)$. Let B be the approximate isotropic bandwidth defined as the radius of the region of k-space coverage. Then the approximate maximum angular separation is

$$\Delta\phi \approx \frac{\Delta u}{B}$$

If the number of samples for each projection are N, $\Delta\phi$ can be written as

$$\Delta\phi \approx \frac{2}{N} \tag{41}$$

From the circular sampling theorem, the minimum value of $\Delta\phi$ is also equal to

$$\Delta\phi = \frac{2\pi}{(2K + 1)} \approx \frac{\pi}{K} \tag{42}$$

Comparing Eq.(41) and (42), a sufficiently high value K for good image reconstruction is

$$K = \frac{\pi N}{2} = 2\pi AB \tag{43}$$

Eq.(43) gives the minimum number of samples in ϕ which need to be taken for good image reconstruction.

In addition to satisfying the conditions mentioned earlier in this section, care has to be taken to minimize the interpolation errors and the errors due to the synthesis of the incident plane wave

reconstruction of the image.

Geophysical tomography is a powerful technique for reconstructing images of underground objects. Although similar to medical computer tomography in principle, it is more complicated due to the diffraction effects which cannot be neglected at the frequencies which are used for geophysical applications. The limited number of viewing angles available also result in deterioration of the image along the direction of gaps in k-space coverage. Despite this and the other limitations mentioned in the earlier sections, images of good quality can be obtained by this technique.

The recipe for reconstructing the image of the subsurface spill using direct interpolation in diffraction tomography can be summarized as follows:

1. Select the various parameters (frequency, receiver spacing, etc.) according to the limitations and the desired performance.
2. Synthesize a plane wave using Eq.(1) and (2).
3. From the Fourier transform of the measured field, evaluate the Fourier transform of the object profile along the semicircular arcs using Eq.(22).
4. Use the chosen interpolation technique to generate the interpolated values of the object profile.
5. Determine the points on the rectangular grid in frequency domain at which the object profile is desired.
6. Convert these points into corresponding (κ, ϕ) coordinates using the transformation equations (28), (29), (33) and (34).
7. Assign the interpolated values to the Fourier transform of the object profile at these points.
8. Take the inverse Fourier transform to obtain the object profile.

Some of the related areas which need further research are the extension of diffraction tomography to strong scatterers and its performance in the presence of an inhomogeneous background, and the effect of polarization.

Resolution", IEEE Trans. Antennas Prop., vol. AP-32, no.10, pp. 1018-1026, 1984.

[4] Devaney, A.J., "Geophysical Diffraction Tomography", IEEE Trans. Geosc. Remote Sensing, vol. GE-22, no.1, pp. 3-13, 1984.

[5] Mueller, R.K., Kaveh, M., and Wade, G., "Reconstructive Tomography and Application to Ultrasonics", Proc. IEEE, vol. 67, no.4, pp. 567-587, 1979.

[6] Chu, T., and Lee, K., "Wide Band Microwave Diffraction Tomography Under Born Approximation", IEEE Trans. Antennas Prop., vol. 37, no. 4, pp. 515-519, 1989.

[7] Pan, S.X., and Kak, A.C., "A Computational Study of Reconstruction Algorithms for Diffraction Tomography: Interpolation Versus Filtered Backpropagation", IEEE Trans. Acoust., Speech, Signal Processing, vol. ASSP-31, no.5, pp. 1262-1275, 1983.

[8] Witten, A.J., and Long, E., "Shallow Applications of Geophysical Diffraction Tomography", IEEE Trans. Geosc. Remote Sensing, vol. GE-24, no.5, pp. 654-662, 1986.

[9] Stark, H., Woods, J.W., Paul, I., and Hingorani, R., "Direct Fourier Reconstruction in Computer Tomography", IEEE Trans. Acoust., Speech, Signal Processing, vol. ASSP-29, no.2, pp.237-245, 1981.

[10] Chew, W.C., "Waves and Fields in Inhomogeneous Media", New York, Van Nostrand Reinhold, 1990.